

SYNTHESIS AND CHARACTERIZATION OF ZnO NANOWIRES BY MOCVD

Chang Soon Huh

Applied Chemistry Major, Division
of Chemical and Environmental
Engineering, College of
Engineering /Dong-eui University
SOUTH KOREA

ABSTRACT

Zinc Oxide (ZnO) nanowires were synthesized by Metal Oxide Chemical Vapor Deposition (MOCVD) system by controlling the particle size of the catalyst involved in growth. The nanowire formation was successfully confirmed by minimizing the time for the process by dipping the wafer into the liquid phase catalyst and reacting directly through CVD. In order to determine the optimal conditions for growth of nanowires (NWs) in the above experiment, the reaction was carried out at various times and temperatures under an argon (Ar) atmosphere. We could observe that the diameter and size of nanowire are increasing as the particle size of the catalyst increased.

Keywords: ZnO nanowires, Metal Oxide Chemical Vapor Deposition (MOCVD), Structural and optical properties.

INTRODUCTION

Ever since the discovery of carbon nanotubes by Iijima [1] in 1991, there has been great interest in the matter or structures at nanoscale so called nanotechnology are widely investigated as the most important challenge for our future. Recently one-dimensional (1D) nanostructures such as wires, rods, belt, and tubes have also become the focus of intensive research owing to their unique applications in mesoscopic physics, optical, electrical transport and fabrication of nanoscale devices [2-11]. For this reason to generate and manipulate nano size structures are big issued these days. Nanotechnology refers to a field of applied science whose theme is the control of matter on an atomic and molecular scale. Generally nanotechnology is approximately 100 nanometres (nm) on smaller and involves developing materials or devices within that size. Progress in nanotechnology necessitates inventing methods to observe, characterize, and control the phenomena at the nanometre-scale. Characterization techniques such as electron microscopy, scanning probe microscopy, and X-ray methods assist in studying materials at nanoscale. Nanoscale measurements are challenging and require tomographic imaging, atomic scale resolution, and scanning over large area [12]. Emergence of the novel characterization techniques such as scanning tunnelling microscopy (STM) and atomic force microscopy (AFM) are few of the reliable method investigate the nanoscale phenomena [13, 14]. Not only, these techniques facilitated the characterization and measurements but also eased the manipulations at the molecular scale. This ability to manipulate can be further enhanced by combining with the techniques such as transmission electron microscopy (TEM) [15]. Recently, STM technique was also used to manipulate the bonding of a molecular species such as carbon monoxide and the structure and vibrational properties of the product were analysed [16]. But the concerns of the temperature, surface diffusion, conductivity of the sample, and precision in the bond

manoeuvring using STM tip are of the high priority. Nanotechnology is a highly multidisciplinary field, drawing from a number of field such as applied physics, materials science, interface and colloid science, device physics, chemical engineering, mechanical engineering, biological engineering, and electrical engineering. Thus, Nanotechnology is interdisciplinary field or fusion technology and science because it requires from basic science (chemistry, physics and life science) to many field of engineering. This wide range science and technology will influence all parts of our lives and will be revolution or new paradigm for our future.

EXPERIMENTAL AND THEORETICAL METHODS

In our laboratory, a high temperature furnace, we deposited Au nanoparticles by the method of MOCVD as a catalyst of NWs. Catalyst metal is of vital importance to achieve the desires nanowire morphology. For ZnO nanowire growth, besides Au (Figure 1), there have been reports on using Sn, Ni, Cu and Se as the catalysts. Metal organic compound has high volatility at moderately low temperature and also control of precursor evaporation rate is relatively easy for liquids. The control of experimental conditions such as furnace temperature, vapour pressure of the precursor in the inert carrier gas has a profound effect on the growth of metal nanoparticles in a uniform scale. Most of MOCVD is done in the UHV environment. Walsh and Bottka deposited Fe films onto GaAs using $\text{Fe}(\text{CO})_5$ at the substrate temperatures of 150 to 300 °C and deposition rates of 0.3 nm/min in a conventional CVD system using hydrogen as the carrier gas [17]. But we heat the furnace up to 960 °C atmosphere pressure to lead small sized metal particle. In order to confirm the presence of significant deposition, we first analysed the morphology with high resolution-scanning electron microscopy (HR-SEM) (Hitachi S-4200, accelerating voltages 0.5 to 30 kV). Because of the deviation of the deposition rate, we cut the samples and labelled them. For the confirmation of effective NWs growth on nano-sized Au particle, we analysed the NWs with



instruments of SEM and TEM (Figure 2).

Figure 1. Images of experimental used all substrates.

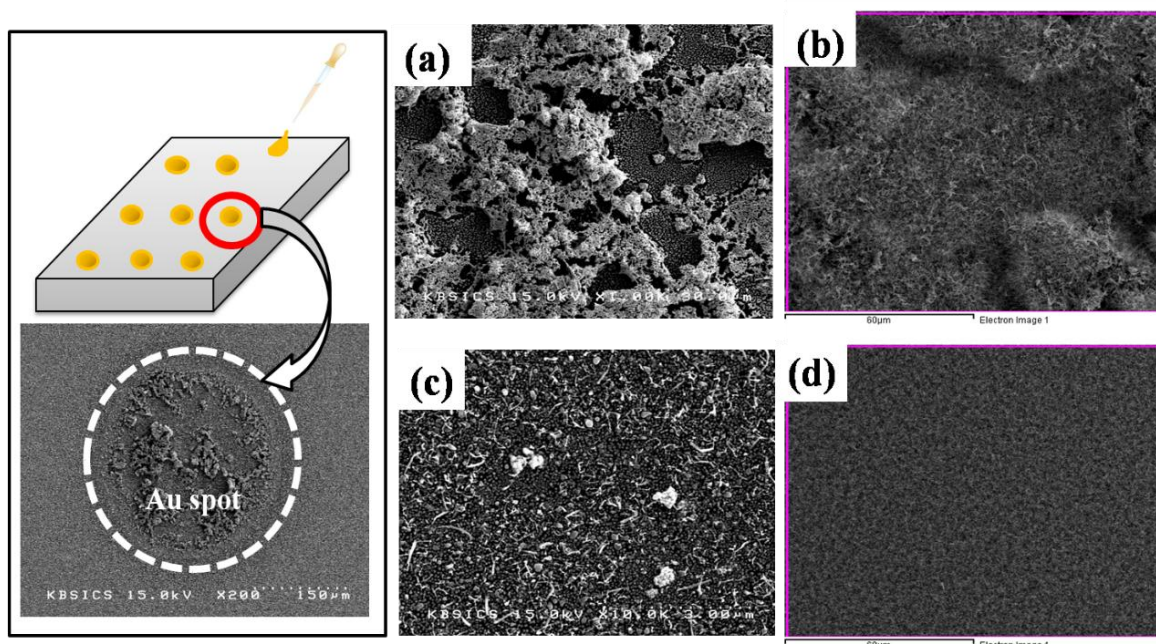


Figure 2. SEM images of (a), (b): taken inside the spot of gold nanoparticles, and (c), (d): surface outside the oxidized silicon surfaces.

RESULTS

We have developed a technique for generating nano metal particles that can be used for catalyst of growing nanowires using various methods. One of this methods experiment of NWs synthesis with gold chloride solutions and hydroxylamine on silicon oxide by solution phase catalyst deposition. Hongjie Dai group suggested the solution phase iron nanoparticles formation on Si wafer and the following single wall nanotubes (SWNTs) synthesizing [18]. The phenomenon of highly efficient deposition of iron containing nanoparticles on SiO_2 from the mixed hydroxylamine and FeCl_3 solution is interesting. Previously, It has been used to Au^{3+} to Au for deposition onto premade colloidal Au nanoparticles (2 to 15nm) and thus for particle enlargement. Brown group [9] reported the size increase of Au nanoparticles exposed to mix Au^{3+} and hydroxylamine is efficient in enlarging preformed nanoparticle and pH being the important reaction elements. (Figure. 3)

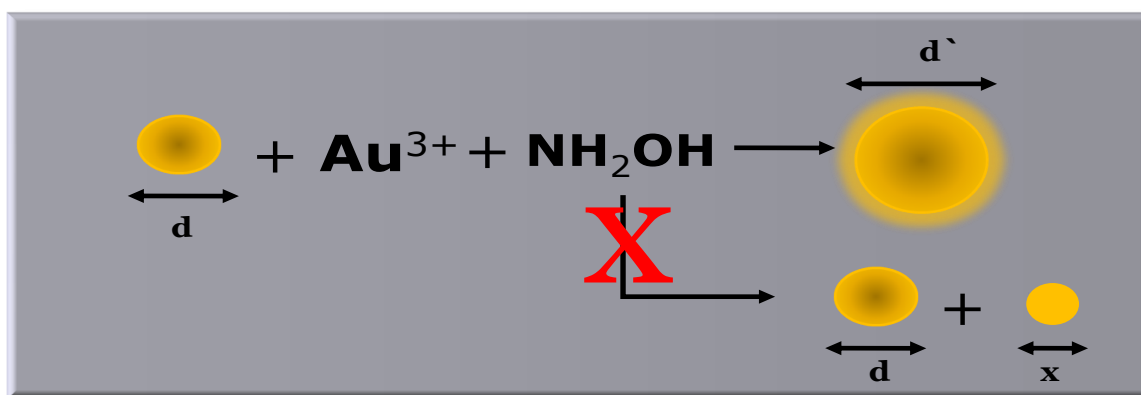
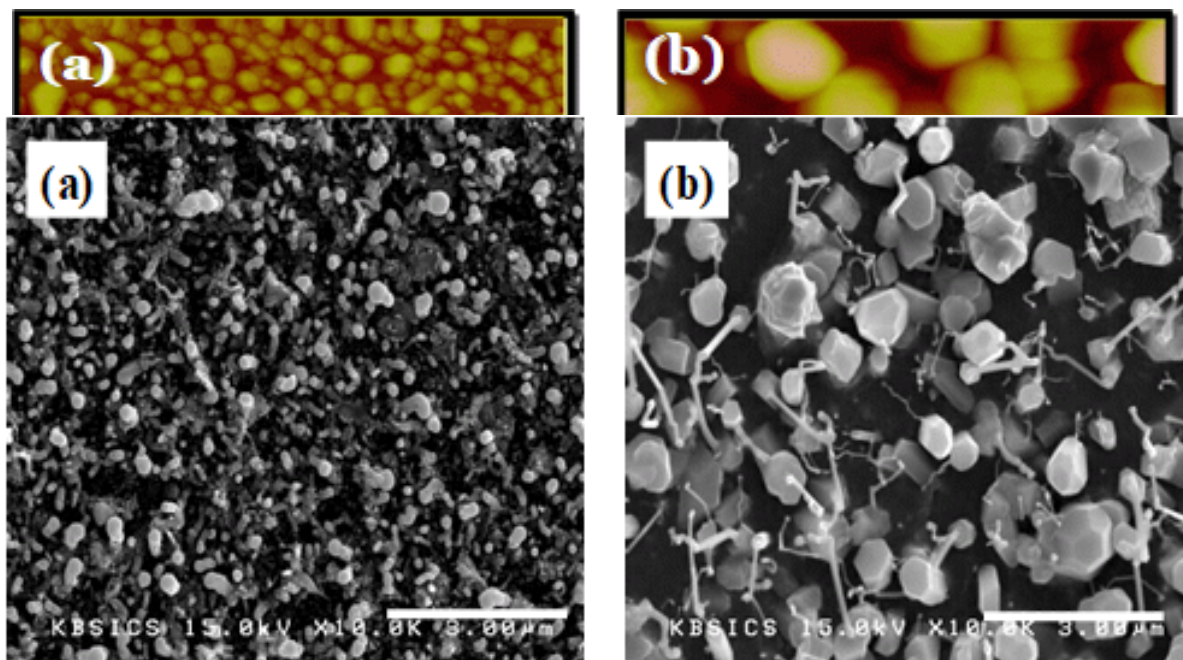


Figure 3. Described herein is a method for enlargement of colloidal Au nanoparticles called “seeding”, based on the colloidal Au surface-catalysed reduction of Au^{3+} by NH_2OH [19].

Consequently, the development of this method offers the possibility of important areas. Figure 4 and Figure 5 shows Au nanoparticles used as seeds in NWs synthesis. The size of particle affects the diameter of NWs and length. The surface property, reaction, and pH of the reaction solutions play equally important roles in the formation of nanoparticles. The particles size and the NWs morphology have been examined using AFM, HR-SEM.

Figure 4. AFM images of (a) Au nanoparticles after calcination on SiO₂ without



hydroxylamine in the gold chloride solution and (b) Au nanoparticles after calcination on SiO₂ surface after dipping in a solution of Gold chloride/0.4mM hydroxylamine.

Figure 5. SEM images of (a) Au nanoparticles after calcination on SiO₂ for 10min and (b) nanoparticles after calcination formed on SiO₂ after soaking in a solution of Gold -chloride / 0.4 mM hydroxylamine for 10min.

And SiO₂ grown Si (p-type) wafer was cleaned with Piranha solution (H₂SO₄:H₂O₂=3:1) and then dried under a N₂ atmosphere. Gold chloride solution (Aldrich), hydroxylamine hydrochloride (98 %, A.C.S. reagent, Aldrich), and DI (deionized) water used. The Au-containing nanoparticles formation was achieved by immersing the SiO₂ substrate into a vial containing 10 mL of water and 10 μL of gold chloride solution, followed by immediate addition of 100 μL of 40 mM NH₂OH·HCl (aq) into the vial. This acid (metal complex) and base reaction is pH dependent and nano size particle is formed at pH 2.5. After a few seconds stirring, the substrate was allowed to soak in the solution for a certain period of time (10 min) before being taken out of the solution, rinsed consecutively with water, acetone, and isopropyl alcohol, and dried. Figure 6 shows ZnO NWs are grown in high yield from the synthesized Au nanoparticles by the thermal CVD method. ZnO NWs were synthesized in a horizontal hot wall two-zone furnace as shown in Figure 7.

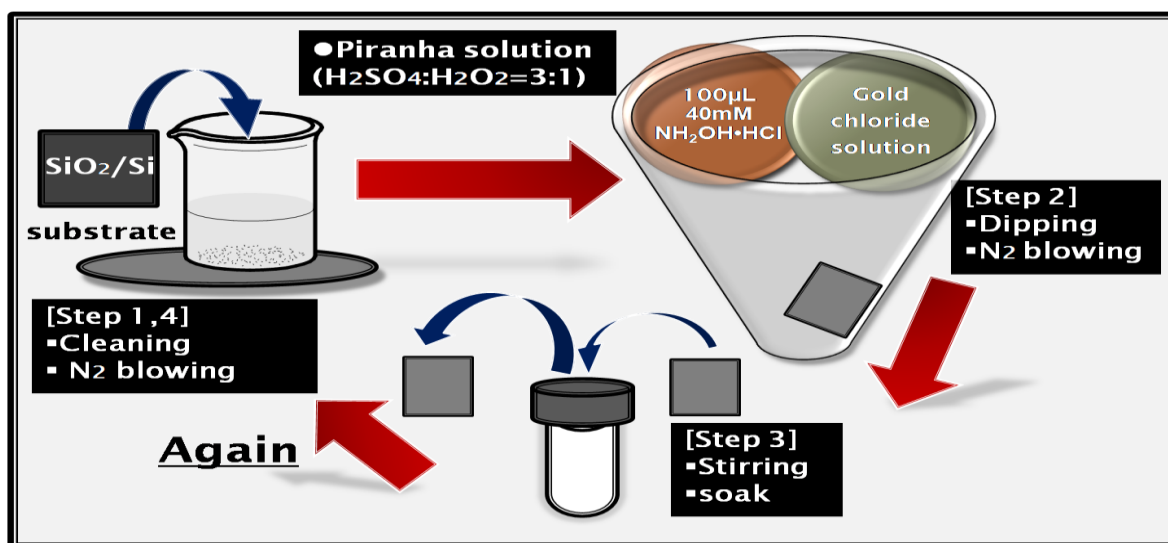


Figure 6. Pre-treatment process for formation of Au nanoparticles on the Si/SiO₂ substrate.

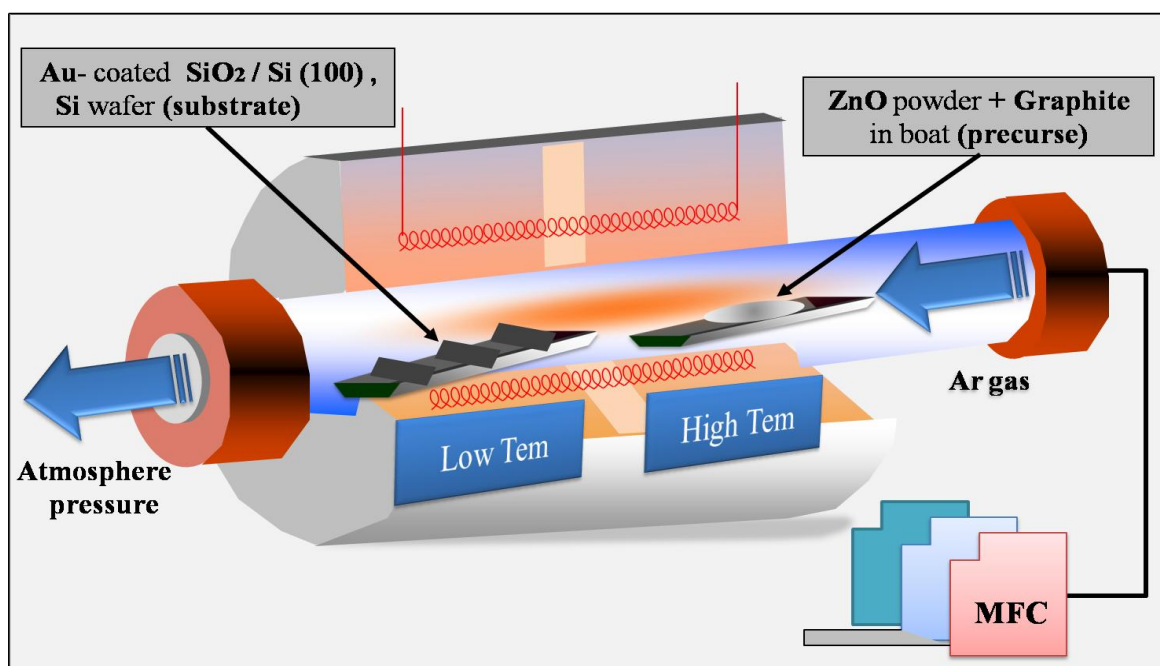


Figure 7. A schematic illustration of the CVD system

The setup is equipped with pressure and mass flow controllers (MFC). The synthetic approach is based on a simple modification of the van-Arkel method, used for the separation or purification of metals through vapour transport. The ZnO powder precursor is evaporated and transported to the higher temperature zone by a carrier gas, where decomposition of ZnO powder and reaction with SiO₂ substrate occurs. The substrates were placed in the middle of the lower temperature zone in a conventional two zone horizontal hot-wall furnace. The ZnO powder precursor was placed in an alumina boat in the middle of the higher temperature zone. The temperatures of two-zones were independently controlled. The higher temperature zone (HT) and lower temperature zone (LT) were used for vaporization of precursor and NW growth, respectively. The substrates were placed at 10 cm from the precursor position in the LT zone. Powders of ZnO (99.0% Aldrich) and graphite mixed in a molar ratio of 1:2 as the source material, was pushed to the middle of the HT zone in the tube. The SiO₂ (p-type) substrate dipped with gold colloid was placed in another alumina boat near the LT zone of the tube. Before heating began, argon was flow into the tube with a flow of 30 Standard Cubic Centimetre per Minute (cm³/min) for a 30min. Then it took about 30min for the temperature in the HT zone to reach 960°C and that around LT zone 440°C accordingly. Finally, the furnace was switched off and the allowed the cool down to room temperature in the tube with the argon gas still flowing. In brief, Schematic depicting the process of experiment are in Figure 8.

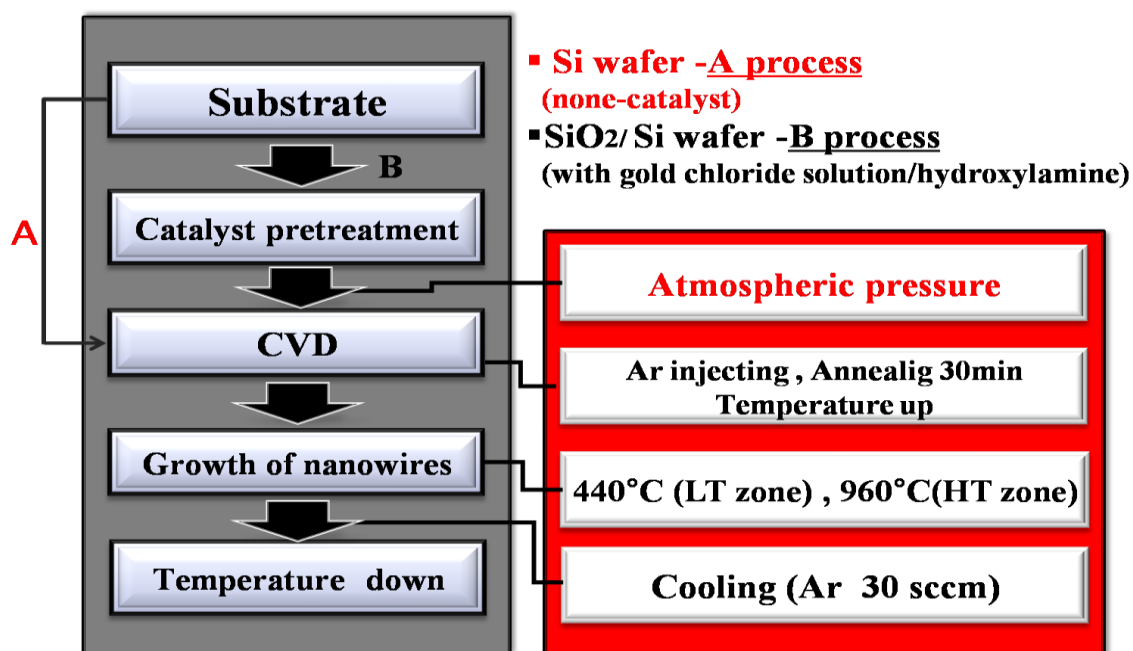
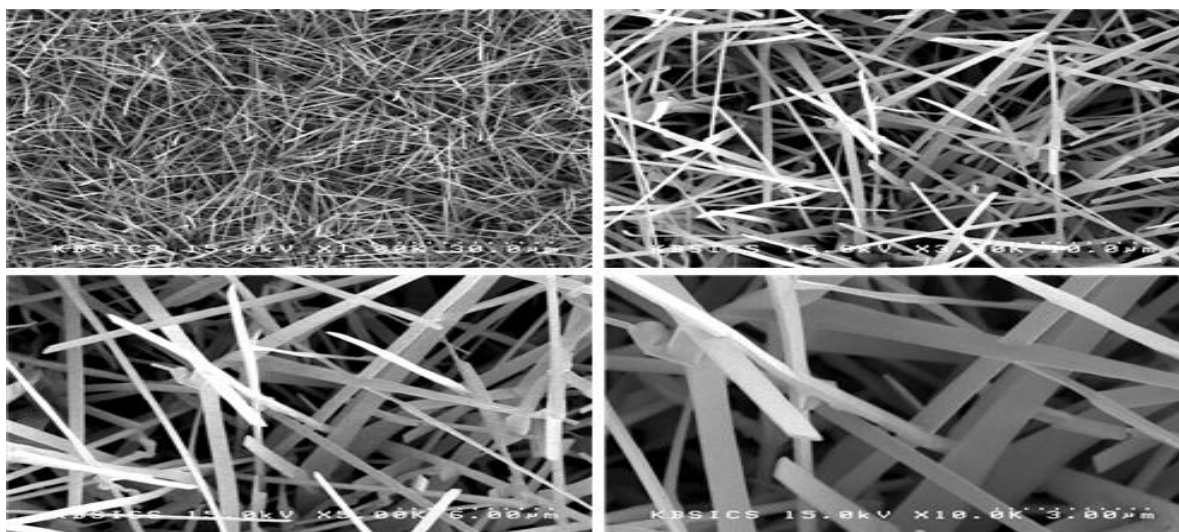


Figure 8. Schematic depicting the process of experiment

DISCUSSION

The morphology of the materials on the substrate was examined by SEM (Hitachi S-4200, accelerating voltages 0.5-30kV). SEM images of the ZnO nanowire arrays grown at a CVD for 30min on Si (100) substrate without catalyst, SiO₂/Si substrate after dipping in the gold chloride solution, SiO₂/Si substrate after dipping in a solution of gold chloride/0.4mM hydroxylamine are shown in Figure 9 to 11, respectively. It can be seen that ZnO nanowires have tapered tips and were vertically aligned on all of the substrates. On the basis of the above analyses, the possible ZnO NWs growth via the self-catalytic mechanism was

proposed since no other catalyst or additive participated in the reaction (Figure 9). And SEM images demonstrate clearly that larger nanocluster catalyst can lead to the reproducible growth of larger diameter and lengthy NWs (Figure 10, 11). The key role of the catalyst in defining the NWs diameter produced by CVD is evident from the analysis of the diameter



distributions.

Figure 9. SEM images of ZnO nanowires deposited on Si (100) substrate without Catalyst.

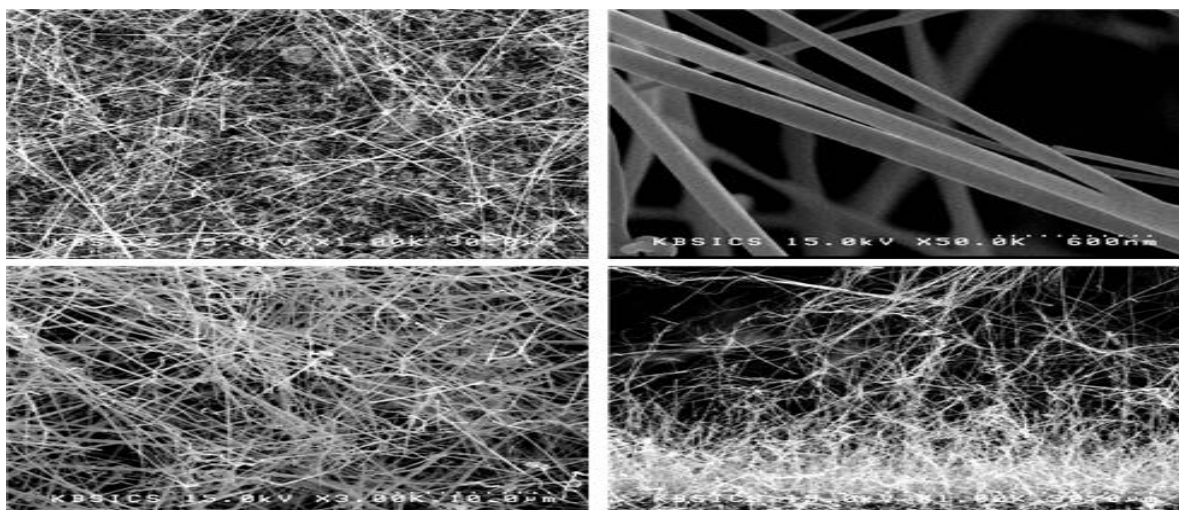


Figure 10. SEM images of ZnO nanowire deposited on SiO₂/Si substrate after dipping in the gold chloride solution.

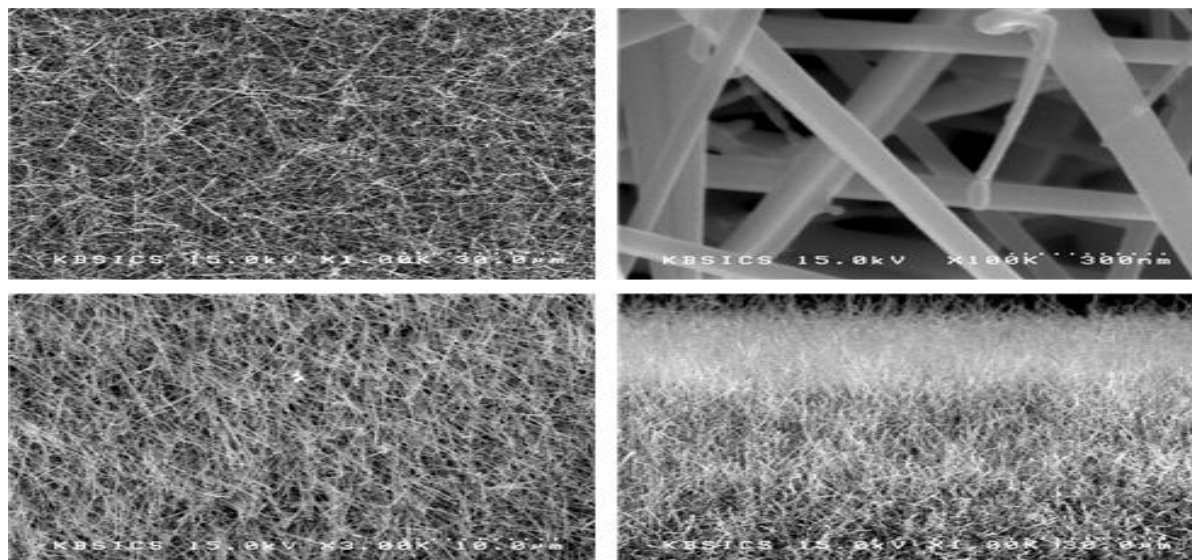


Figure 11. SEM images of ZnO nanowire deposited on SiO₂/Si substrate after dipping in a solution of Gold chloride/0.4mM hydroxylamine.

Figure 12 shows the typical x-ray diffraction spectra (XRD) (1.2kW Cu K α , $\lambda=1.54\text{\AA}$) of these ZnO NWs (JCPDS card No. 800075). This spectra can be indexed for diffraction from the (100), (002), (101), (102), and (103) planes of wurtzite crystals with lattice constants $a=0.325\text{nm}$ and $c=0.521\text{nm}$, which are corresponding to ZnO. The dominant (002) of non-catalyst ZnO peak indicates that these ZnO NWs are grown along the c-axis direction since these nanostructures are partially vertically aligned on the substrate. In addition to diffraction peaks from the Au catalysts, no other peaks due to impurity phases were observed. In the case of using Au catalysts, the diffraction pattern (111) of the NWs shows, and a much higher (002) peak intensity compared with that observed in ZnO powder diffraction, which has its maximum intensity for the (101) peak. This change in intensity pattern for the NWs is consistent with the NWs growing nearly vertically on the substrate and along the c-axis in the cases of Au catalysts. In fact if the nanowires were perfectly vertically aligned on substrates and grew perfectly along the c-axis, only the diffraction peaks from the (00 l) plane could be observed in the XRD pattern. Energy-dispersive spectroscopy (EDS) identifies that the composition of the NWs is Zn, O, and Au in Figure 13. The Au content is about 9.54 atom %.

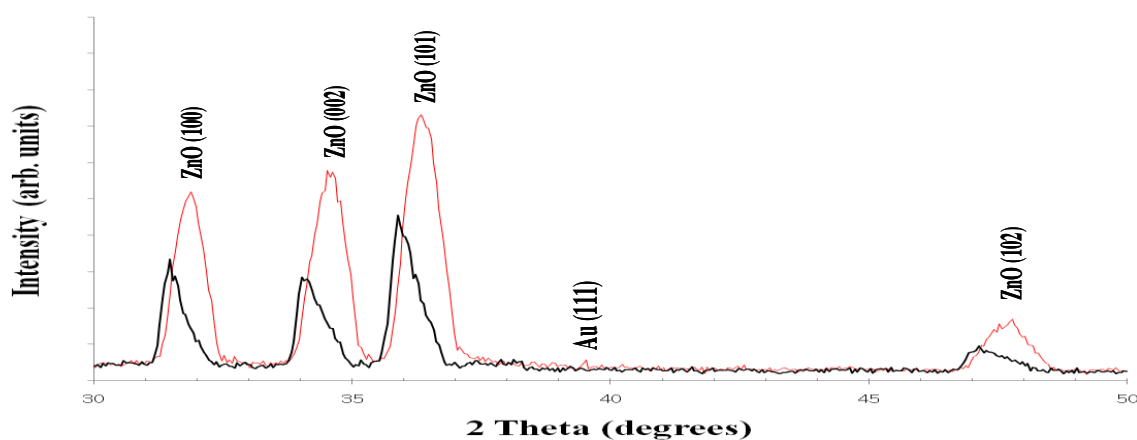


Figure 12. XRD patterns of un-doped and Au-doped ZnO nanowires.

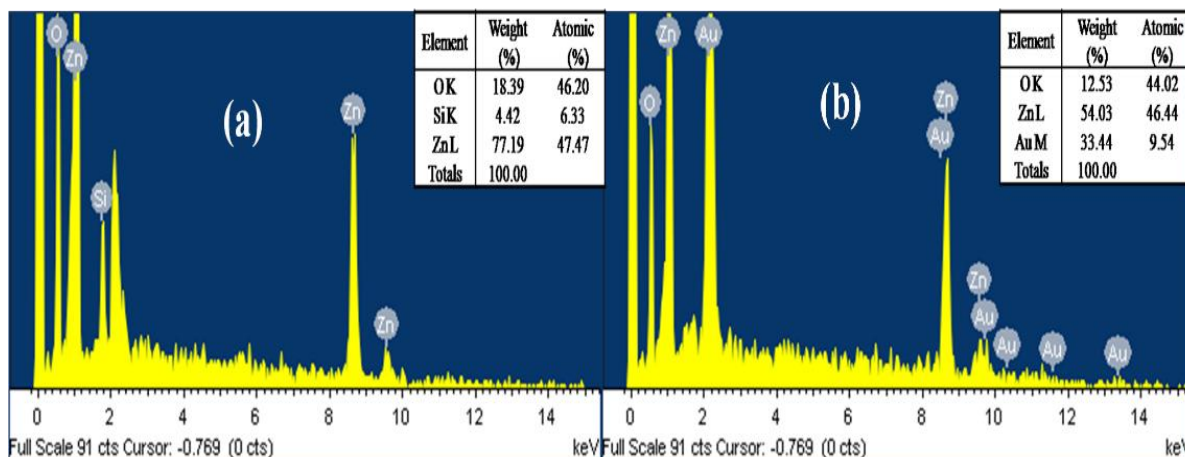
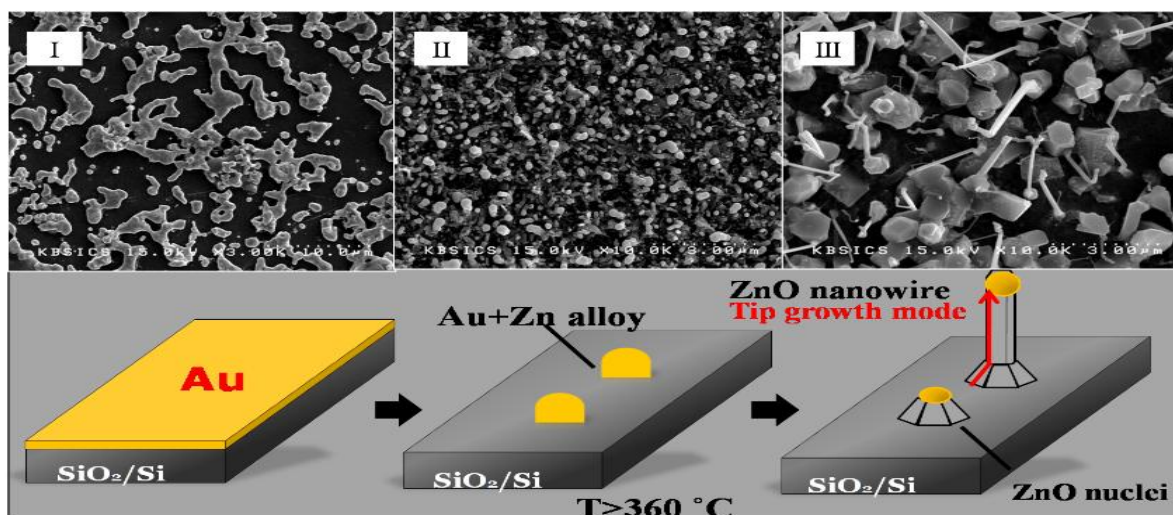


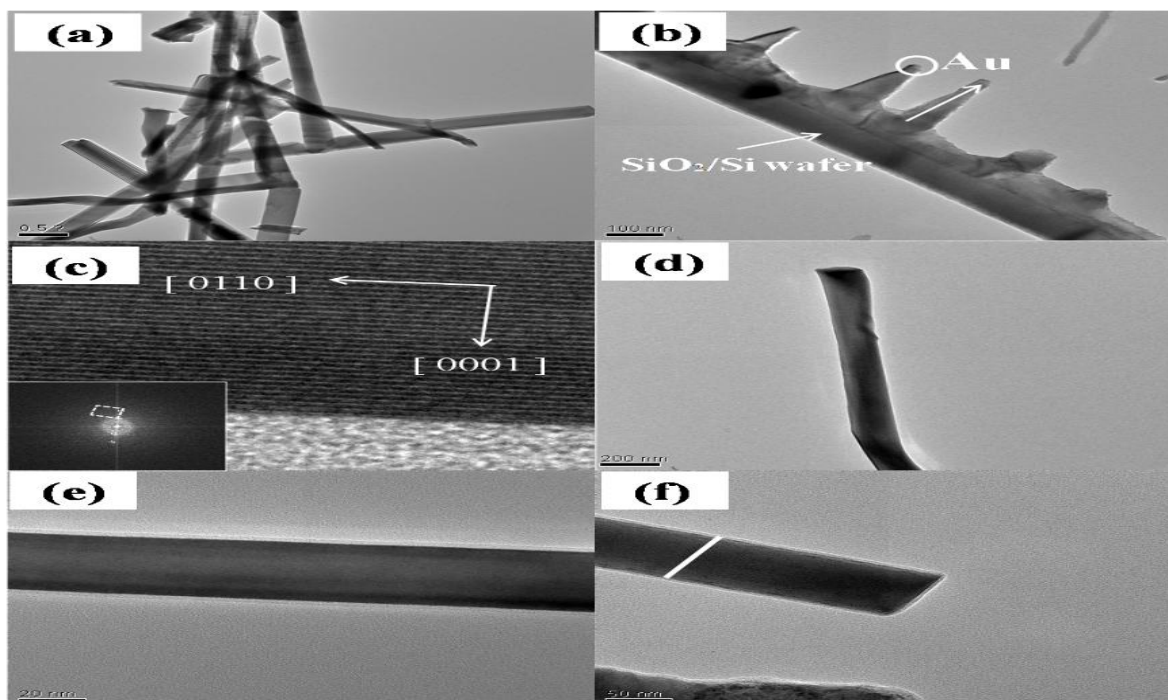
Figure 13. EDX spectra of the face on Si (100) wafer (a), and SiO₂/Si wafer with Au catalyst particles (b)

The TEM (JEM 2011, accelerating voltage range 80 to 200 kV) image representing the general morphology of the ZnO NWs is displayed in Figure 14(a). It shows that the NWs are straight. Figure 14(b) shows ZnO NWs deposited on SiO₂/Si substrate. Figure 14(c) shows the high-resolution TEM (HR-TEM) image. The selected-area ED (SAED) pattern shows that a single-crystalline ZnO NWs showing the lattice with the [0110] direction parallel to the long axis. Figure 14(d) shows a thin ZnO NWs with a Zn/Au alloy tip. The presence of the alloy tip is indicative of a growth process by the VLS mechanism. Such tips have been found for NWs grown by both the graphite and hydrogen reduction methods (Figure 15). Figure 14(e) shows the TEM image of ZnO NWs on SiO₂/Si wafer with Au catalyst particles. The average diameter of the NWs is 40 nm. Figure 14(f) shows the TEM images of ZnO NWs on SiO₂/Si substrate after dipping in a solution of Gold particles. The average diameter of the NWs is 50



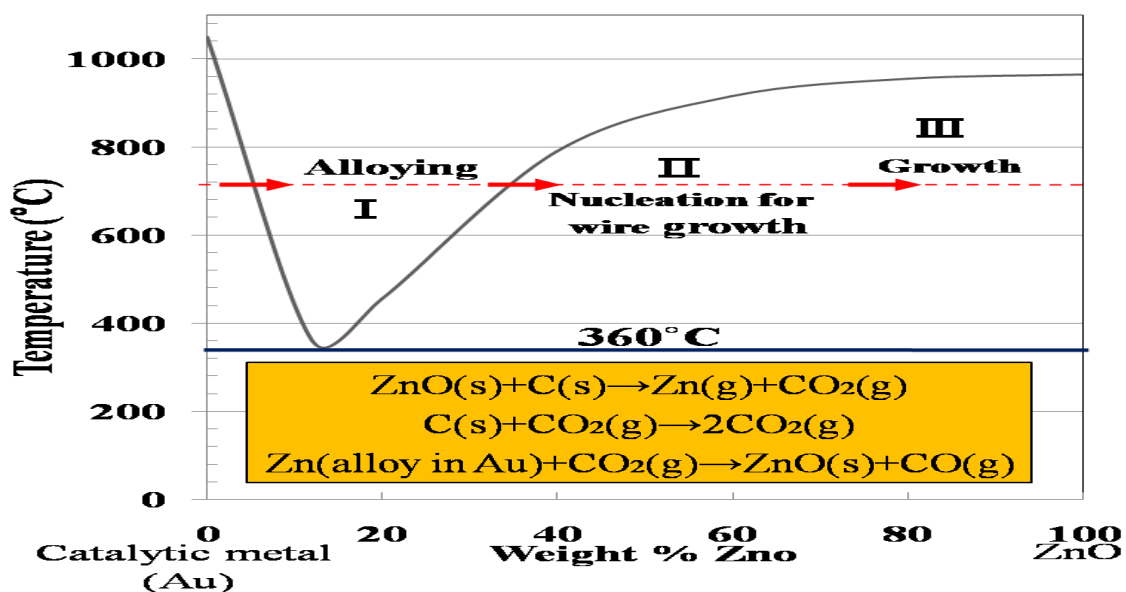
nm.

Figure 14. (a) TEM image show the general morphology of the ZnO NWs. (b) TEM images of ZnO NWs deposited on SiO₂/Si substrate. (c) HRTEM images for the ZnO NWs, showing the (0110) fringes perpendicular to the growth direction. The SAED pattern is given in the inset which shows the nanowire is single crystalline with [0110] growth direction. (d) TEM image of a thin ZnO NWs with a Zn/Au alloy tip. (e) TEM image of ZnO NWs on SiO₂/Si wafer with Au catalyst particles. (f) TEM images of ZnO



NWs on SiO₂/Si substrate after dipping in a solution of Gold chloride/0.4mM hydroxylamine.

(A)

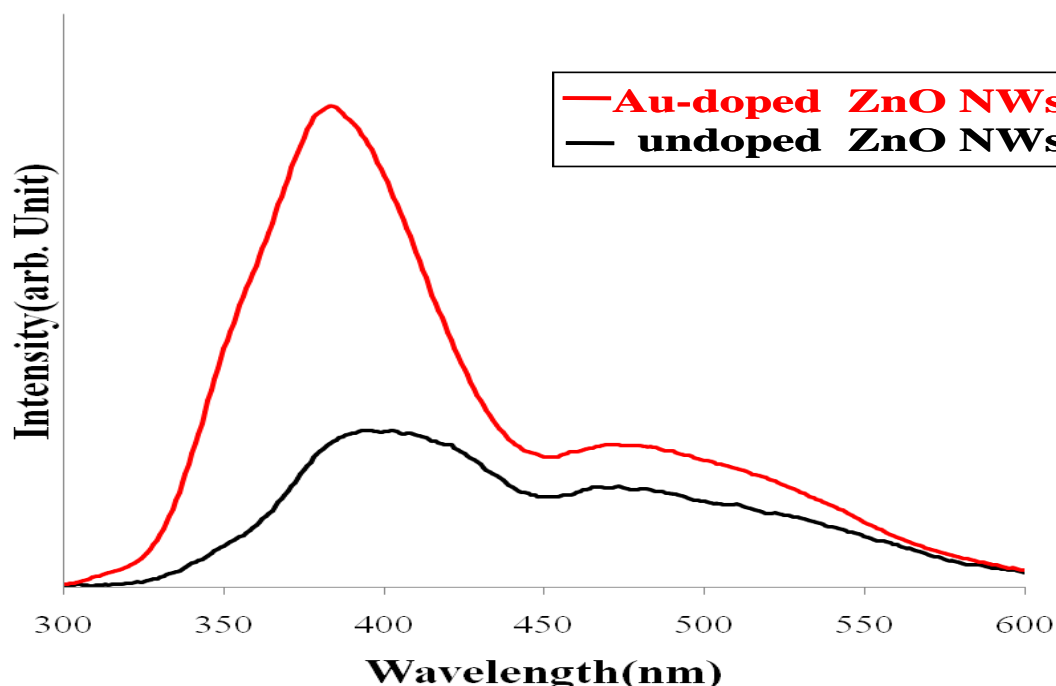


(B)

Figure 15. (A) SEM images of Au catalyst particles. And proposed growth processes for the nanowire via the vapor-liquid-solid (VLS) mechanism. (B) The binary phase diagram between Au and ZnO, with an indication of the compositional zones responsible for alloying, nucleation, and growth.

Furthermore, these samples were also analysed by Photoluminescence (PL) as excited by a He-Cd laser (wavelength at 325nm). Figure 16 shows the PL spectrum measured at room temperature. Two typical emission peaks at 380 to 500 nm were observed, which were

assigned to UV emission and green emission while at the UV emission corresponds to the nearest band-edge emission (NBE), the green emission peak is commonly referred to as a deep-level or trap-state emission. We also observed increasing all emission intensity (380 to 500 nm) when using the Au catalyst. That is, the emission of PL thinks the NWs sizes. A predominant emission peak near 380 nm is observed and corresponds to the recombination of the free excitons. In addition a weak broad emission (green emission) near 500nm is attributed to intra band defect levels including the singly ionized oxygen vacancy in ZnO. The progressive increase of the green light emission intensity relative to the UV emission as the wire diameter decreases suggests that there is a greater fraction of oxygen vacancies in



the thinner nanowires.

Figure 16. Photoluminescence spectra of ZnO nanowires.

CONCLUSIONS

ZnO NWs were successfully organized various thin film formation methods by the growth nucleic. Thereafter the particle formation by low temperature annealing (360 °C ~ 400 °C) examined by AFM (Atomic force microscopy) measurement. Au nanoparticles used as seeds in ZnO NWs synthesis. We had experiment of NWs synthesis with gold chloride solutions and hydroxylamine on silicon oxide by solution phase catalyst deposition. Previously, it has been reported the size increase of Au nanoparticles exposed to mixing Au³ and hydroxylamine is efficient in enlarging preformed nanoparticles. The development of this method offers the possibility of important areas. The controlled size of particle affects the diameter and length of NWs. The surface property, reaction, and pH of the reaction solutions play equally important roles in the formation of nanoparticles. We tried to synthesize ZnO NWs are grown in high yield from the synthesized. Samples were analysed by SEM, XRD, EDS, AFM, TEM, and PL.

ACKNOWLEDGEMENTS

This work was supported by a research grant from Dong-Eui University.

REFERENCES

- [1] S. Iijima. (1991) Helical microtubules of graphitic carbon. *Nature* 354, 56-58.
- [2] A. N. Banerjee, (2011) The design, fabrication, and photocatalytic utility of nanostructured semiconductors: focus on TiO₂-based nanostructures. *Nanotechnol. Sci. Appl.* 4, 35–65
- [3] V. C. Anitha, A. N. Banerjee & S. W. Joo. (2015) Recent developments in TiO₂ as *n*- and *p*-type transparent semiconductors: synthesis, modification, properties, and energy-related applications. *J. Mater. Sci.* 50, 7495–7536.
- [4] Steel, B. C. H. & Heinzl, A. (2001) Materials for fuel-cell technologies. *Nature* 414, 345–352.
- [5] S. M. Choi, J. H. Kim, J. Y. Jung, E. Y. Yoon & W. B. Kim. (2008) Pt nanowires prepared via a polymer template method: its promise toward high Pt-loaded electrocatalysts for methanol oxidation. *Electrochim. Acta* 53, 5804–5811.
- [6] A. Morozan, P. Jegou, B. Jusselme, S. Palacin. (2011) Electro chemical performance of annealed cobalt–benzotriazole/CNTs catalysts towards the oxygen reduction reaction. *Phys. Chem. Chem. Phys.*, 13, 21600-21607.
- [7] B.C.H. Steele, A. Heinzl. (2001) Materials for fuel-cell technologies. *Nature*, 414, 345-352.
- [8] K. Kinoshita, J.T. Lundquist, P. Stonehart. (1973) Potential cycling effects on platinum electrocatalyst surfaces. *J. Electroanal. Chem. Interfacial Electrochem.* 48, 157-166.
- [9] T. Ioroi, Z. Siroma, N. Fujiwara, S. Yamazaki, K. Yasuda. (2005) Highly Stable and Active Pt/Nb-TiO₂ Carbon-Free Electrocatalyst for Proton Exchange Membrane Fuel Cells. *Electrochem. Commun.* 7, 183-188
- [10] N. Marcovic, H.A. Gasteiger, P.N. Ross, X. Jiang, I. Villegas, M.J. Weaver. (1995) *Electrochim. Acta.*
- [11] K. Wang, H.A. Gasteiger, N.M. Marcovic, P.N. Ross Jr. (1996) *Electrochim. Acta*, 41, 2587.
- [12] M. C. Gupta, (2002), Mechanisms of shock-induced reactions in high explosives. *AIP Conference Proceedings*, 615, 14.
- [13] G. Binning, H. Rohrer, C. Gerber, E. Weibel. (1982) Materials for fuel-cell technologies *Physical Review Letters* 49, 57.

- [14] G. Binning, C. F. Quate, C. Gerber, (1986) Atomic Force Microscope. *Physical Review Letters* 56, 930.
- [15] D. B. Williams, C. B. Carter. (1996) Transmission electron microscopy, *Plenum Press, New York*, Vol. 1.
- [16] H. J. Lee, W. Ho, (1999), Single-Bond Formation and Characterization with a Scanning Tunneling Microscope. *Science*, 286, 1719.
- [17] P. J. Walsh, N. Bottka. (1984) Growth of Fe and FeAs₂ Films on GaAs by Organo-Metal Chemical Vapor Deposition Using Pentacarbonyl Iron and Arsine. *J. Electrochem Soc.* 131, 444.
- [18] M. Ohring, (2002), *Materials Science of Thin Films 2nd Ed*: Academic Press, San Diego, 608.
- [19] H. Dai et al. (2003) Efficient Formation of Iron Nanoparticle Catalysts on Silicon Oxide by Hydroxylamine for Carbon Nanotube Synthesis and Electronics. *Nano Lett.* 3, 157-161.